JGR Biogeosciences

RESEARCH ARTICLE
10.1029/2019JG005242

Sensitivity of Methane Emissions to Later Soil Freezing in Arctic Tundra Ecosystems

Kyle A. Arndt[1,2], Walter C. Oechel[1,3], Jordan P. Goodrich[4,1], Barbara A. Bailey[5], Aram Kalhori[1], Josh Hashemi[1,2], Colm Sweeney[6], and Donatella Zona[1,7]

[1]Global Change Research Group, San Diego State University, San Diego, CA, USA, [2]Department of Land, Air, and Water Resources, University of California Davis, Davis, CA, USA, [3]Department of Geography, College of Life and Environmental Sciences, University of Exeter, Exeter, UK, [4]Scripps Institute of Oceanography, University of California, San Diego, La Jolla, CA, USA, [5]Department of Mathematics and Statistics, San Diego State University, San Diego, CA, USA, [6]Earth System Research Lab, NOAA, Boulder, CO, USA, [7]Department of Animal and Plant Sciences, University of Sheffield, Sheffield, UK

Key Points:
- During the last two decades soil has been freezing later in the Arctic (from 2001-2017)
- The presence of unfrozen soils are associated with sustained emissions of methane until January in tundra ecosystems
- Air temperature does not capture soil conditions in the fall, and shallow soil temperature underestimates the duration of unfrozen soils

Supporting Information:
- Supporting Information S1

Correspondence to:
K. A. Arndt,
karndt-w@sdsu.edu

Citation:
Arndt, K. A., Oechel, W. C., Goodrich, J. P., Bailey, B. A., Kalhori, A., Hashemi, J., et al. (2019). Sensitivity of methane emissions to later soil freezing in Arctic tundra ecosystems. *Journal of Geophysical Research: Biogeosciences*, *124*, 2595–2609. https://doi.org/10.1029/2019JG005242

Received 6 MAY 2019
Accepted 4 AUG 2019
Accepted article online 12 AUG 2019
Published online 29 AUG 2019

Abstract The atmospheric methane (CH_4) concentration, a potent greenhouse gas, is on the rise once again, making it critical to understand the controls on CH_4 emissions. In Arctic tundra ecosystems, a substantial part of the CH_4 budget originates from the cold season, particularly during the "zero curtain" (ZC), when soil remains unfrozen around 0 °C. Due to the sparse data available at this time, the controls on cold season CH_4 emissions are poorly understood. This study investigates the relationship between the fall ZC and CH_4 emissions using long-term soil temperature measurements and CH_4 fluxes from four eddy covariance (EC) towers in northern Alaska. To identify the large-scale implication of the EC results, we investigated the temporal change of terrestrial CH_4 enhancements from the National Oceanic and Atmospheric Administration monitoring station in Utqiaġvik, AK, from 2001 to 2017 and their association with the ZC. We found that the ZC is extending later into winter (2.6 ± 0.5 days/year from 2001 to 2017) and that terrestrial fall CH_4 enhancements are correlated with later soil freezing (0.79 ± 0.18-ppb CH_4 day^{-1} unfrozen soil). ZC conditions were associated with consistently higher CH_4 fluxes than after soil freezing across all EC towers during the measuring period (2013–2017). Unfrozen soil persisted after air temperature was well below 0 °C suggesting that air temperature has poor predictive power on CH_4 fluxes relative to soil temperature. These results imply that later soil freezing can increase CH_4 loss and that soil temperature should be used to model CH_4 emissions during the fall.

Plain Language Summary Methane (CH_4) is a powerful greenhouse gas, capturing more heat per molecule than carbon dioxide (CO_2). Although CH_4 is less concentrated in the atmosphere, it is the second most important greenhouse gas with respect to climate change after CO_2. Arctic tundra ecosystems are potentially major sources of CH_4, given large soil carbon storage and generally wet conditions, favorable to CH_4 production. This study investigates if the persistence of unfrozen soils is associated with higher CH_4 emissions from the Arctic. We combined long-term soil temperature measurements, terrestrial CH_4 enhancements from the National Oceanic and Atmospheric Administration monitoring station in Utqiaġvik, AK, and CH_4 emissions from Arctic tundra ecosystems across four stations in the North Slope of Alaska. Our results show that from 2001 to 2017 the soil is freezing later and that later soil freezing is associated with higher fall CH_4 enhancements. Given that unfrozen soils are related to higher CH_4 emissions, a later soil freezing could contribute to the observed increase in the regional atmospheric CH_4 enhancement. Unfrozen soil layers persisted after the air temperature was well below 0 °C, suggesting that air temperature does not properly predict the sensitivity of CH_4 emissions to climate warming.

1. Introduction

The Arctic is subjected to a series of warming-induced positive feedbacks that have accelerated regional warming compared to the global average, referred to as polar amplification (IPCC, 2013). The largest temperature change in the Arctic has been reported outside the typical June–August growing season, leading to warmer winters (Bekryaev et al., 2010). Methane (CH_4) emissions outside of the growing season, including during the fall zero curtain (ZC, when soils remain unfrozen near 0 °C (Hinkel et al., 2001; Outcalt et al., 1990)), can represent the dominant component of the annual budget (Pirk et al., 2016; Treat, Bloom, &

Marushchak, 2018; Zona et al., 2016). The ZC period includes the early part of the cold season (September to November) but can persist even later (December and January) in some years and sites (Hinkel et al., 2001; Outcalt et al., 1990). Multidecadal observations of CH_4 fluxes from Arctic ecosystems would be ideal to identify the response of CH_4 fluxes to Arctic warming. However, studies of fall CH_4 emissions are sparse and inconsistent (Mastepanov et al., 2008; Mastepanov et al., 2013; Pirk et al., 2015; Sturtevant et al., 2012; Tagesson et al., 2012) or are of short duration (Taylor et al., 2018; Zona et al., 2016) limiting our understanding of the impact that ZC duration and dynamics have on CH_4 emissions from Arctic ecosystems.

Given the extensive organic carbon stored in Arctic soils (Hugelius et al., 2014), if even a fraction of this carbon reservoir is released as CH_4 or CO_2 (1–4 Pg C-CH_4 by 2100 based on various Representative Concentration Pathway scenario 2.6–8.5 (Schuur et al., 2013)), this carbon could have a substantial effect on the global climate (Schuur et al., 2013; Schuur et al., 2015). However, there is still disagreement on the contribution of high-latitude wetlands to the recent renewed growth in atmospheric (CH_4; Crill & Thornton, 2017; Poulter et al., 2017), making it critical to understand the controls on underlying processes in order to predict changes in the global CH_4 budget. While CH_4 emissions from high-latitude wetlands are currently only about 4% of global CH_4 emissions and 15% of the emission from natural wetlands (Kirschke et al., 2013), increases in area, thaw period, and temperature could further increase their contribution (Zhang et al., 2017). Isotope analyses have shown a negative shift in $\delta^{13}CH_4$ associated with the renewed increase in CH_4 concentrations since 2007, suggesting rising contributions from biogenic sources rather than fossil fuel use and extraction (Kirschke et al., 2013; Nisbet et al., 2016). However, there is still debate over the contribution of different ecosystems to the increase (Poulter et al., 2017; Saunois et al., 2016). Top-down estimates based on atmospheric inversion models (which use transport models to identify the sources and the emissions of CH_4) estimate much lower CH_4 loss than bottom-up estimates (based on site-level measurements upscaled to a larger region using remote sensing products and modeling; Kirschke et al., 2013).

Despite the tie between microbial processes and CH_4 fluxes (Ho et al., 2014; Lipson et al., 2013; Yavitt et al., 2011), many models do not take microbial abundances into account (Nazaries et al., 2013). Methanogens, which create CH_4, are more prevalent at depth (Wagner et al., 2017), which is the opposite of methanotrophs, which consume CH_4 and exist closer to the surface. One of the primary reasons for the microhabitat differences within the soil has to do with the soil water content (Freitag et al., 2010) where methanotrophs require oxygen and methanogens are anaerobic. Because of microbial dependence on the presence oxygen, soil moisture content can be a good predictor of variability in surface CH_4 fluxes (McLain et al., 2002). There is a lack of studies on the microbial communities during the fall shoulder season; however, we hypothesize that communities located deeper in the soil, containing methanogens, may still be active and producing CH_4 after surface soils, where methanotrophs are found, have frozen.

An increase in the CH_4 concentration above background levels (i.e., CH_4 enhancement) of 0.69 ± 0.36 ppb per year over the last two decades has been observed in Utqiaġvik (formerly Barrow), Alaska, during late fall/early winter (November and December, hereby indicated as fall), mostly due to substantial recent anomalies (Sweeney et al., 2016). Sweeney et al. (2016) used air temperature to understand the impact of warming on the terrestrial fall CH_4 enhancement because a consistent long-term time series of soil temperature from Utqiaġvik is not available. However, no relationship was found between rising air temperatures and Arctic CH_4 enhancements after September (Sweeney et al., 2016). Methane production and emission are highly temperature dependent (Dunfield et al., 1993), but microbial soil respiration continues well below freezing, even if at lower rates, and has been observed down to −18 °C (Elberling & Brandt, 2003). Given this temperature dependence, we hypothesize that CH_4 emissions are consistently higher before soil freezing across all our sites due to the higher production and release. As soils freeze, emissions are still possible through cracks (Mastepanov et al., 2013; Pirk et al., 2015), sometimes attributed to the gas in the soil column becoming pressurized (Tagesson et al., 2012), but we expect these emissions to be higher than after soil freezing. As the soil remains unfrozen after the air temperature is well below 0, we also hypothesize that air temperature does not properly capture the persistence of unfrozen soil layers, which is associated to higher CH_4 emissions. Finally, we hypothesize that later soil freezing contributes to the increase in the terrestrial CH_4 enhancement observed in Utqiaġvik over the last decade and that this process might have a larger-scale impact with continued climate change.

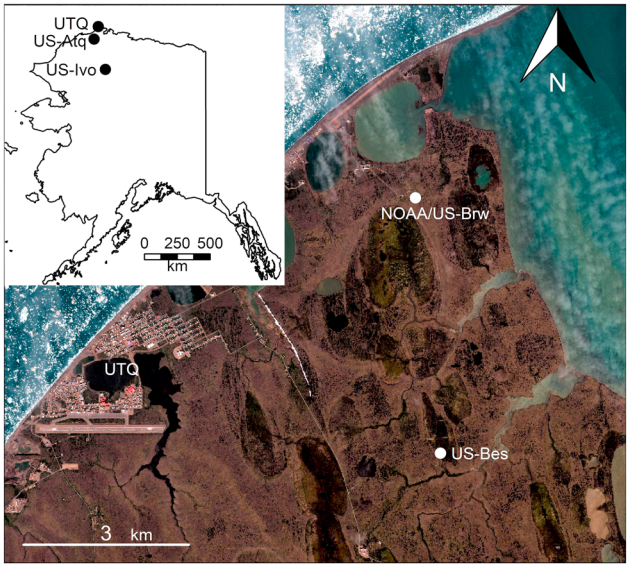

Figure 1. WorldView-2 (Digitalglobe™) true color image of the Utqiaġvik (UTQ) region and an AK map inset showing the location of the eddy covariance tower sites and National Oceanic and Atmospheric Administration (NOAA) BRW station in Alaska. The map was made in R (R Core Team, 2018) using a true color RGB WorldView2 (DigitalGlobe™) image collected 20 July 2016 and a shapefile of the state of Alaska from the U.S. Census Bureau. Graphical features and functions are from the "raster" (Hijmans, 2018), "rgdal" (Bivand et al., 2018),"gridBase" (Murrell, 2014), and "prettymapr" (Dunnington, 2017) R packages.

2. Materials and Methods

2.1. Study Sites

Four sites across the North Slope of AK were used for this study (Figure 1 and Table 1); two of these sites are in Utqiaġvik (indicated as UTQ in Figure 1): US-Brw (Zona & Oechel, 1998) and US-Bes (https://ameriflux.lbl.gov/sites/siteinfo/US-Bes). US-Brw is the farthest north tower in Utqiaġvik and is colocated with the National Oceanic and Atmospheric Administration (NOAA) Earth System Research Laboratory (ESRL, site name BRW, Figure 1). US-Brw has relatively low soil moisture (Table 1), and the vegetation is dominated by graminoids (Kwon et al., 2006). US-Bes is the control site of the Biocomplexity Manipulation Experiment, is in a drained lake basin dominated by wet sedges (Zona et al., 2009), and is inundated for much of and sometimes all of the growing season. Atqasuk (US-Atq, Zona & Oechel, 1999) is about 100 km south of Utqiaġvik at a warmer polygonised site. Much of the landscape consists of a mixture of tussock tundra and shrubs with some sedges (Davidson, Santos, et al., 2016), and the soil at the US-Atq site is sandy (Walker et al., 1989). Ivotuk (US-Ivo, Zona & Oechel, 2003) is about 300 km south of Utqiaġvik in the northern foothills of the Brooks Range and is the southernmost site. US-Ivo is characterized as a mixed tussock tundra/moss composition and is gently sloped (Davidson, Santos, et al., 2016).

2.2. Eddy Covariance

Eddy covariance (EC) CH_4 fluxes and meteorological data were collected from the four towers (Table 1 and Figure 1). Half-hourly CH_4 fluxes were calculated from high frequency (10 Hz) data using EddyPro® (LICOR®, USA). The following procedures were followed in the flux processing: A double rotation was applied to the axis rotations of three-dimensional wind speeds (Wilczak et al., 2001) and a block-averaging interval was used to define turbulent fluctuations; time lags between vertical wind speed and gas concentrations were compensated by maximizing the covariance. The Los Gatos Research (ABB Group, USA) Fast Greenhouse Gas Analyzer (LGR FGGA), a closed path gas spectrometer, was used at all sites except US-Ivo where there was no grid power and the open path LI-COR® LI-7700 was used. Anemometers used are as follows: US-Brw, Metek uSonic-3 (METEK Meteorologische Messtechnik GmbH, Germany); US-Bes and US-Atq, CSAT3 (Campbell Scientific®, USA); and US-Ivo, Metek uSonic-3 Class A (METEK Meteorologische Messtechnik GmbH, Germany). A cross-comparison between the LGR

Table 1
Locations of the Flux Tower Sites and Instruments Used

Site	DOI/URL	Coordinates	Height (m)	CH_4 IRGA	Sonic Anemometer	Air temp. (°C)	Soil temp. (°C)	VWC (%)
US-Brw	doi:10.17190/AMF/1246041	71.3225 N −156.6091 W	4.17	LGR FGGA	Metek uSonic-3	−9.25 ± 11.43	−4.82 ± 6.78	47 ± 7
US-Bes	https://ameriflux.lbl.gov/sites/siteinfo/US-Bes	71.2808 N −156.5964 W	2.20	LGR FGGA	CSAT3	−9.09 ± 11.96	−3.42 ± 7.18	83 ± 20
US-Atq*	doi:10.17190/AMF/1246029	70.4696 N −157.4089 W	2.42	LGR FGGA	CSAT3	−9.40 ± 13.62	−4.26 ± 7.18	41 ± 15
US-Ivo New Location*	doi:10.17190/AMF/1246067	68.4805 N −155.7568 W	3.42	LI-7700	Metek uSonic-3	−6.38 ± 13.44	−0.80 ± 5.95	72 ± 23
US-Ivo Old Location		68.4864 N −155.7502 W			Class A	−8.18 ± 14.08	−0.16 ± 5.54	73 ± 27

Note. Values represent the mean value ± the standard deviation over the course of the flux data used (2013–2017). The US-Ivo values were split from the date of the tower move so that values before 16 June 2016 are included in the old location, and values after 9 July 2016 (when the tower was operational again) are the new location. Soil moisture (VWC) was only assessed when soil temperature was above freezing to avoid skewing the data due to frozen soils where all sites fall near 0%. Asterisk (*) indicates a site with a high-resolution soil profile. IRGA = infrared gas analyzer; LGR FGGA = Los Gatos Research Fast Greenhouse Gas Analyzer; VWC = volumetric water content.

Table 2
ZC Start and End Days for the Four Sites Used in This Study

	Zero curtain end day (Julian day)							
	US-Brw		US-Bes		US-Atq		US-Ivo	
Year	Start	End	Start	End	Start	End	Start	End
2001	234	257	—	—	—	—	—	—
2002	276	306	—	—	—	—	—	—
2003	253	285	—	—	—	—	259	313
2004	257	299	—	—	256	293	255	296
2005	263	276	264	303	252	295	243	295
2006	264	309	264	312	264	309	231	293
2007	276	308	—	—	269	294	265	269
2008	270	311	258	317	—	—	—	—
2009	—	—	309	309	—	—	—	—
2010	—	—	267	329	—	—	—	—
2011	267	314	—	—	263	295	—	—
2012	225	323	277	340	252	304	—	—
2013	—	—	261	345		—	242	359
2014	—	—	264	328	263	322	245	339
2015	261	298	254	301	253	301	242	335
2016	250	306	256	321	256	308	305	324
2017	263	317	271	361	306	320	240	358

Note. A soil depth of −5 cm was used at all sites except US-Bes where −10 cm was used due to data coverage and availability. Start and end days are represented by days on the Julian calendar. Em dash (—) represents a data gap where the end of the ZC_{SH} could not be determined. ZC = zero curtain.

FGGA and the LI-COR® LI-7700 assured comparability of the results across sites using different instruments (Goodrich et al., 2016). For the LI-7700 at US-Ivo, a Webb, Pearman, and Leuning correction was applied according to Webb et al. (1980). The high-pass filtering effect was corrected according to Moncrieff et al. (2005), and a fully analytic low-pass filter correction was applied to the open path raw data (Moncrieff et al., 1997). An in situ/analytic correction (Ibrom et al., 2007) was applied to the closed path data.

Additional postprocessing was performed using the following criteria: The initial quality check was done following Mauder and Foken (2011) where low-quality data indicated with a quality flag of "2" were removed. For sites with LGR FGGAs, fluxes where internal instrument chamber pressure was greater than or equal to 155 torr (20.7 kPa) were removed as it indicated instrument failure. A turbulence threshold (U*) was also applied where data with U* less than 0.1 m/s were removed (Reichstein et al., 2005). A moving window of 2 weeks was applied, and fluxes that were three standard deviations away from the mean were removed as outliers.

2.3. Meteorological Measurements

The air temperature (measured using an HMP 45, Vaisala, Finland) and soil temperature (measured using type T or E thermocouples, Omega Engineering, USA) from each respective site were used for the statistical analysis of the weekly averaged CH_4 fluxes. Soil volumetric water content (VWC; i.e., soil moisture) was measured using Campbell Scientific® CS616 water content reflectometers. Soil moisture probes were either parallel buried in the soil at the same depth as the thermocouples, (−5 cm at US-Atq and US-Ivo) or were inserted from the surface to 10-cm depth at US-Bes and US-Brw, where digging was prohibited. Meteorological data were recorded on Campbell Scientific® CR23X data loggers at all sites except US-Ivo where a Campbell Scientific® CR3000 data logger was used. Measurements were made every 5 s and recorded in half-hourly means. The air temperature recorded at the NOAA site was used for the analysis of the relationship with the CH_4 enhancement. Soil temperatures for the four towers sites were used for defining the ZC start and end date in the time series analysis (Table 2). For all the analyses using soil temperatures, measurements collected at −5-cm depth (negative values represent distances below the soil surface) were used for all sites except US-Bes where soil temperature measurements from −10 cm were used due to better data availability. All ZC designations using this shallower depth are hereby defined as ZC_{SH} for "ZC shallow." In summer 2016, we installed two high spatial and temporal resolution temperature profiles at the US-Atq and US-Ivo sites to better characterize the soil freezing and the persistence of unfrozen soils during the cold period (Arndt et al., 2019). A third was installed at the US-Bes site during summer 2018 (Arndt et al., 2019). These profiles included thermocouples every 5 cm from 25 cm above the surface to 90 cm below the surface at US-Ivo and US-Atq and 75 cm below the surface at US-Bes (Table 3 and Figure 2). All ZC designations referring to the full soil profile or this deeper soil data set are hereby referred to as ZC_F for "ZC full." Data were recorded on a CR6 data logger (Campbell Scientific®) with four AM25T multiplexers (Campbell Scientific®) at US-Ivo and US-Atq and a CR1000 data logger (Campbell Scientific®) with three AM25T (Campbell Scientific®) multiplexers were used at the US-Bes site. The thermocouples measured temperatures at 2 Hz; the half-hour average of these measurements was recorded. ZC estimations that apply to both will not include the subscripts.

ZC conditions were designated as the period when daily mean soil temperatures were between 0.75 and −0.75 °C consistent with that reported in Zona et al. (2016). The start of the ZC was defined as the first day to meet the ZC conditions after the growing season (i.e., spring thaw was not considered in this study), and the end of the ZC was defined as the last day meeting the mentioned criteria. We realize that the shallower soil depths may underestimate the duration of the ZC_F compared to the deeper high-resolution soil temperature profile (Table 3). Unfortunately, we were forced to use the soil temperature data from −5-

Table 3
Results Comparing the Weekly Mean CH_4 Flux Rates From the Eddy Covariance Towers During the ZC_{SH} and After Soil Freezing at the Four Eddy Covariance Sites From 2013–2017

Site	Median flux rates ± standard deviation (mg C-CH_4·m^{-2}·hr^{-1}) During	N	After	N	*p* value
US-Atq	0.21 ± 0.04	18	0.15 ± 0.07	17	0.02
US-Bes	0.40 ± 0.09	23	0.11 ± 0.09	23	<0.001
US-Brw	0.42 ± 0.14	18	0.21 ± 0.13	22	<0.001
US-Ivo	0.82 ± 0.44	53	0.4 ± 0.23	38	<0.001

Note. There was a significant decrease in the CH_4 flux rates after soils froze. A Wilcox rank-sum test was used to assess the *p* value. ZC = zero curtain.

and −10-cm depths to model the long-term changes in the ZC_{SH} duration from 2001 to 2017 in place of the high-resolution profile system, as these shallower soil temperature data were the only ones available across the whole time period used for estimating the decadal change in the ZC duration.

2.4. Methane Enhancement Estimates

To identify some of the large-scale implications of our site level measurements, we investigated the temporal change of CH_4 enhancements from the terrestrial area south of Utqiaġvik, obtained from NOAA's Global Greenhouse Gas Reference Network in Utqiaġvik (BRW, 71°19′N, 156°36′W). The NOAA station samples CH_4 concentrations from a 16-m-high tower north of Utqiaġvik. Methane enhancements were estimated by subtracting the monthly mean concentration when wind originated from the clean air sector (0–90°) from the hourly mean CH_4 concentrations of the land sector (150–210°) to estimate the terrestrial contribution as described in Sweeney et al. (2016). Any data with a mean hourly wind speed less than 3 m/s were removed to minimize the effect of local sources (Sweeney et al., 2016) before binning the data into daily mean enhancements. The terrestrial CH_4 enhancements used in this and other studies have been shown to be a good representation for processes occurring not only locally around Utqiaġvik but even further south on the North Slope of AK (Commane et al., 2017; Jeong et al., 2018; Sweeney et al., 2016).

2.5. Statistical Analysis

Linear mixed effect models (LMEs) were used to analyze the change over time in the ZC_{SH} end date (LME_{ZC}, and LME_{ST} and LME_D testing the start date and duration), the fall CH_4 enhancement as a function of the ZC_{SH} end date from 2001–2017 at the four tower sites (LME_{CH4}), and the fall CH_4 fluxes as a function of soil temperature (LME_{soil}) or air temperature (LME_{air}). LMEs are advantageous because they allow for a robust assessment of the relationship between fixed variables (e.g., CH_4 emissions and soil freezing date) while accounting for the "random" effects of replication across different groups or sites and time (Pinheiro & Bates, 2000). LME_{CH4} was also fitted with an AR1 (autoregressive lag 1) structure to address possible temporal autocorrelations. A mixed effects model was used to assess the ZC end date as a function of the VWC (LME_{VWC}) at the four tower sites from 2013 to 2017, when VWC data were collected. The mean VWC recorded the day before the ZC_{SH} conditions started was used in the soil moisture model since VWC drops near-zero percent during and after soil freezing. Therefore, this was deemed as representative of conditions immediately before freeze-up.

To evaluate the statistical differences in the CH_4 fluxes during and immediately after the end of the ZC_{SH}, CH_4 fluxes during the ZC_{SH} period and an equivalent amount of time after the end of the ZC_{SH} were used to evaluate the CH_4 fluxes after the complete soil freezing. Fluxes during July, August, and an equivalent time before the ZC_{SH} were also analyzed. A Wilcoxon rank-sum test was used evaluate differences in mean CH_4 fluxes during the ZC_{SH} period and after the end of the ZC_{SH} for each site separately. A Kruskal-Wallis test was used for the test including the summer period with a post hoc paired Wilcoxon rank-sum test. The nonparametric rank-sum test was used given the sometimes-skewed distribution of the CH_4 fluxes. For the limited period (2013–2017) when both the EC CH_4 fluxes and the atmospheric CH_4 enhancements were available, we tested if weekly atmospheric CH_4 enhancements could be explained as a function of the weekly mean flux rates recorded by the EC towers. Because the CH_4 enhancement was representative of an aggregate of different ecosystem types and flux rates observed at our towers, a mean weekly flux rate across towers was used to analyze the relationship between the CH_4 flux and CH_4 enhancement. Given the heteroscedasticity of the data, an ordinary least squares regression was not appropriate for this analysis. Therefore, a weighted generalized least squares model (using the "nlme" package in R (Pinheiro et al., 2018)) was used to assess the relationship, which is robust with heteroscedastic data (Carroll, 2017; Carroll & Ruppert, 1982).

Given the end date of the ZC_{SH} significantly increased over the 16-year period, the ZC_{SH} and CH_4 enhancements were detrended to meet the assumptions of stationarity and independence in LME_{CH4}. A least squares linear model was used for detrending, where the predicted value was subtracted from the actual value (i.e.,

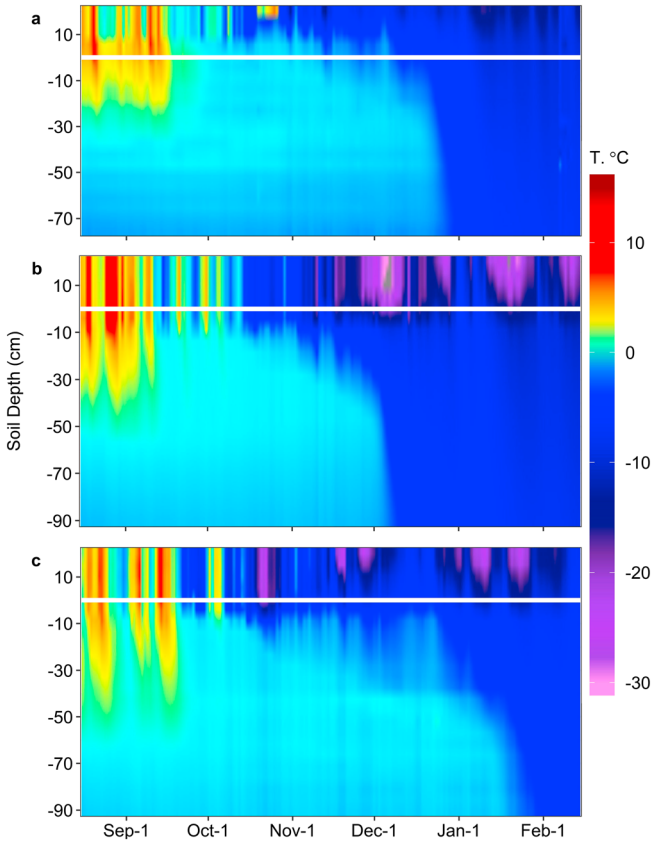

Figure 2. Soil temperatures measured with thermocouples every 5 cm at US-Bes, US-Atq, and US-Ivo (a, b, and c, respectively) to show ZC_F relationships at depth. The ZC_F, represented by cyan, shows freezing fronts from the top and bottom of the soil profile. Data collection of these high-resolution profiles began in 2016 at US-Atq and US-Ivo and 2018 at US-Bes. ZC_F conditions existed into December or January for all three sites for the recent years depicted even as air temperatures were well below freezing. Due to data gaps related to power or equipment failure, years represented are 2018, 2016, and 2017 for a, b, and c, respectively, where data were consistent across the entire ZC_F. ZC = zero curtain.

the residuals of the least squares linear model). Before accepting the LMEs, we also tested the parameters for autocorrelation or partial autocorrelation that might bias the relationship between time series data. Residuals were further examined for temporal autocorrelations to ensure the assumption of individual samples was met. The fall air temperature data were regressed with the fall CH_4 enhancement data using an ordinary least squares regression as model residuals were independent and normally distributed.

LME_{soil} and LME_{air} were used to assess the relative importance of air and soil temperature in explaining the variability of the weekly mean CH_4 flux rates across the four flux tower sites from 2013 to 2017 during the fall. These LMEs included year and site as random effects and air or soil temperature as the fixed effect. Model performance was estimated by comparing the random effect model (that only included the random effects of site and year) and the random intercept and slope model (that included random effects, and the soil or air temperature as a fixed effect), using maximum likelihood estimation. Models were compared using analysis of variance. The correlation coefficients for mixed effects models were calculated using the "r.squaredGLMM" function from the R package "MuMIn" (Barton, 2018). Two R^2 values are reported for LMEs, the marginal (R^2_m) and conditional (R^2_c) representing the correlation coefficient of the fixed effects and whole model, respectively (Nakagawa et al., 2017). All statistical analyses were performed using R (R Core Team, 2018). Additional resources used in the supporting information are Xenakis (2016) and Kormann and Meixner (2001).

3. Results

3.1. Temporal Changes in ZC Duration

Using the long-term soil temperature measurements, we found the ZC_{SH} ended significantly later over the course of the study (the results of LME_{zc} showed $p < 0.001$, $R^2_m = 0.37$, $R^2_c = 0.45$, $N = 44$, Table 2 and Figure 3) with soil freezing occurring 2.6 ± 0.5 days later per year from 2001 to 2017. The start date of the ZC_{SH} did not shift significantly over the course of the study (LME_{ST}, $p = 0.48$, $R^2_m = 0.01$, $R^2_c = 0.01$, $N = 44$, Table 2 and Figure S1). Due to the shift in the end date and the stability of the beginning of the ZC_{SH}, the total duration increased (LME_D, $p = 0.002$, $R^2_m = 0.20$, $R^2_c = 0.25$, $N = 44$, Figure S2). Soil VWC was a significant control on the end of the ZC_{SH} as found by LME_{VWC} showing that soils froze 0.48 ± 0.20 days later per year per %VWC ($p = 0.02$, $R^2_m = 0.32$, $R^2_c = 0.33$, $N = 15$). When analyzing the extent and duration of the ZC_F using high-resolution soil temperature profiles, we observed that soil layers between about −5- and −75-cm depths remained unfrozen after the freezing of surface soils when air temperatures were well below 0 °C (Figure 2). Overall, the soil remained unfrozen until December and sometimes into January across a variety of our sites (Figures 2 and 3 and Table 2). The ZC_F end date was 16, 51, and 96 days later at US-Bes, US-Atq, and US-Ivo, respectively, than the end estimated using soil temperature at −5 cm in the same high-resolution profile (Figure 2). Sites with higher soil moisture content (US-Bes and US-Ivo) had a later soil freeze over the long-term record (Table 2) where US-Ivo and US-Bes froze around 14 November ± 30 days and 20 November ± 18.7 days, respectively, while drier sites like US-Brw or US-Atq on average froze around 28 October ± 17.8 days and 31 October ± 10.6 days.

3.2. Influence of Soil Freezing on CH_4 Fluxes and Terrestrial CH_4 Enhancement

To analyze the effect of soil freezing (ZC_{SH}) on CH_4 emission rates, we compared CH_4 emissions before and after soil freezing using 12 site years from the four EC towers. The weekly mean CH_4 flux rate was consistently significantly higher during the ZC_{SH} than after soil freezing across all four EC tower sites from

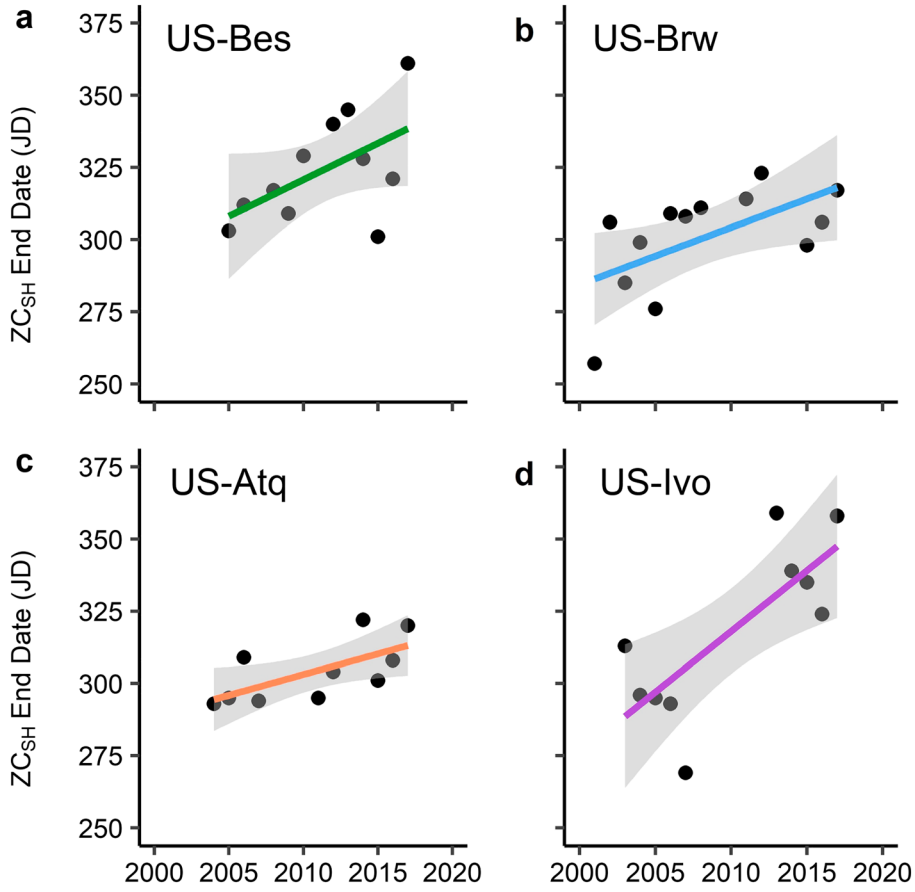

Figure 3. There was a significant increase in the end day of the ZC_{SH} over the course of the study across the four tower sites (panels a–d): assessed using a linear mixed effects model (LME_{ZC}, $p < 0.001$, $R^2_m = 0.37$, $R^2_c = 0.45$, $N = 44$). However, a longer data record is needed to make a strong assertion about this relationship, especially given data gaps. Shaded region represents a 95% confidence interval. ZC = zero curtain.

2013 to 2017 (Figure 4 and Table 3, $p = 0.02$ at US-Atq and $p < 0.001$ the other three sites). All sites displayed a sudden drop in the CH_4 flux rate immediately following soil freezing (Figures 4 and 5). August rates were higher than ZC_{SH} rates ($p < 0.05$); however, the ZC_{SH} rates were sometimes not statistically different from other growing season rates at US-Brw and US-Ivo (Figure S3). The southernmost site (US-Ivo) presented the highest CH_4 emissions after soil freezing across all 5 years with a median flux rate of 0.82 ± 0.44 mg $C\text{-}CH_4 \cdot m^{-2} \cdot hr^{-1}$ (median ± standard deviation, Figure 4). The before freezing flux rates were similar across the Utqiaġvik sites with mean flux rates of 0.40 ± 0.09 mg $C\text{-}CH_4 \cdot m^{-2} \cdot hr^{-1}$ and 0.42 ± 0.14 mg $C\text{-}CH_4 \cdot m^{-2} \cdot hr^{-1}$, respectively, for US-Bes and US-Brw. US-Atq exhibited the lowest efflux rates across of our sites with a median flux rate of 0.21 ± 0.04 mg $C\text{-}CH_4 \cdot m^{-2} \cdot hr^{-1}$ during the ZC_{SH}.

The detrended end date of the ZC_{SH} and the detrended atmospheric CH_4 enhancement from 2001–2017 were significantly correlated (the results of LME_{CH4} showed $p < 0.001$, $R^2_m = 0.29$, $R^2_c = 0.29$, $N = 41$, Figure 6), with the fall CH_4 enhancement increasing by 0.79 ± 0.18 ppb (slope ± standard error) for every day increase in the ZC_{SH} duration. LME_{CH4} was found to have an AR1 structure which did not change results when addressed in the correlation structure of the model. The relationship between the detrended CH_4 enhancement as a function of the detrended ZC_{SH} end date at the US-Bes and US-Ivo sites were independently significant when assessed using ordinary least square models (US-Bes: $p = 0.04$, $R^2 = 0.37$, $N = 10$, Figure 6a; US-Ivo: $p = 0.02$, $R^2 = 0.44$, $N = 10$, Figure 6d). We found a significant positive correlation between the atmospheric CH_4 enhancements and the weekly mean CH_4 fluxes and using the weighted generalized least squares regression (Figure 7, $p < 0.001$, $R^2 = 0.45$, 115.3 ± 13.9-ppb CH_4 enhancement per mg

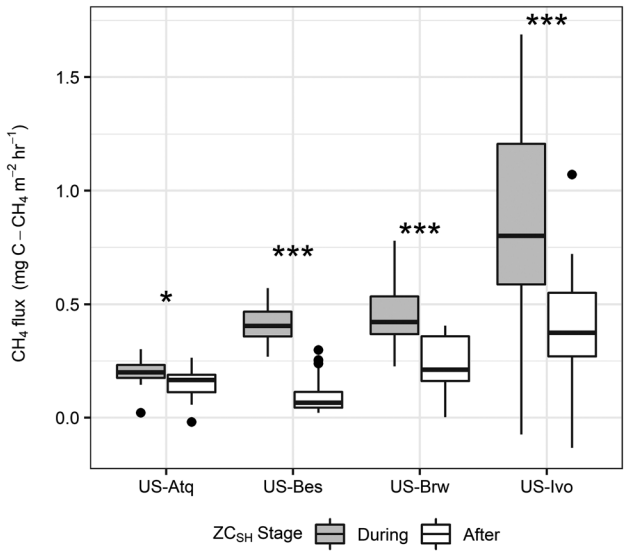

Figure 4. Weekly mean CH_4 flux rates during and after the ZC_{SH} from 2013–2017. During the ZC_{SH}, emission rates are significantly higher at all sites ($p = 0.02$ at ATQ and $p < 0.001$ at the other three sites). ZC = zero curtain.

C-CH_4·m^{-2}·hr^{-1} mean flux rate). Conversely, the fall air temperature did not display a significant correlation with the terrestrial fall CH_4 enhancement ($p = 0.17$, $R^2 = 0.07$, $N = 16$) over the period of the study (2001–2017).

3.3. Role of Soil Temperature on CH_4 Emission Rates After the ZC

Soil temperature (at the −5- and −10-cm depths for consistency with the long-term change in the ZC_{SH}) was a more important predictor on fall CH_4 emissions and on the terrestrial CH_4 enhancement than air temperature. Soil temperature explained 34% of the variability in the weekly mean CH_4 fluxes during the cold season, as compared to air temperature, which only explained 15% of the variability in the fluxes (Table 4). We tested LME_{air} and LME_{soil} comparing CH_4 fluxes as a function of either air or soil temperature versus a null model of CH_4 fluxes as a function of only the random effects (year and site). While models including either air and soil temperature were significant at this scale, soil temperature exhibited a higher explanatory power on the CH_4 fluxes (Table 4).

4. Discussion

In our study, we found fall CH_4 emissions to be higher during ZC_{SH} conditions than after soil freezing across all sites and years measured (2013–2017 for the four EC tower sites). This is consistent with the temperature dependence of CH_4 production that has been well documented in incubation experiments (Dunfield et al., 1993). The temperature sensitivity of CH_4 production has been found to be different below freezing than above freezing (Tucker, 2014), which could aid in explaining why there is a sudden drop in CH_4 emissions after soil freezing (Figures 4 and 5). We observed the warmest site (US-Ivo) to have the highest flux rates both before and after freezing (according to the ZC_{SH} evaluation). However, US-Atq, which is the next warmest has the lowest flux rates, likely due to low soil moisture (~40% VWC) and sandy soils (Walker et al., 1989) providing poor habitat for CH_4 production despite higher temperatures. Sandy soils can further allow higher

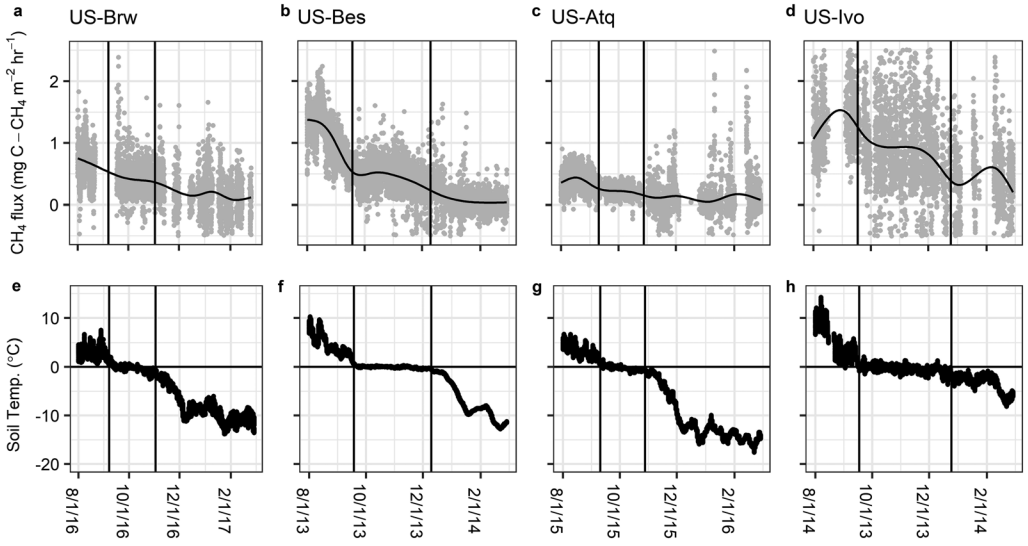

Figure 5. Examples of the decline of CH_4 emissions at the four sites during the ZC_{SH}. The top row (a–d) displays CH_4 fluxes measured by the eddy covariance towers and the bottom row is soil temperature of the corresponding tower (e–h). Vertical bars represent the start and end of the ZC_{SH} where a plateau-like trend exists in the soil temperature and CH_4 fluxes before declining to lower winter temperatures and CH_4 emission rates with occasional bursts. Fluxes peak in the warm growing season and decline until the ZC_{SH} where fluxes continue at sustained rates until the soil fully freezes. ZC = zero curtain.

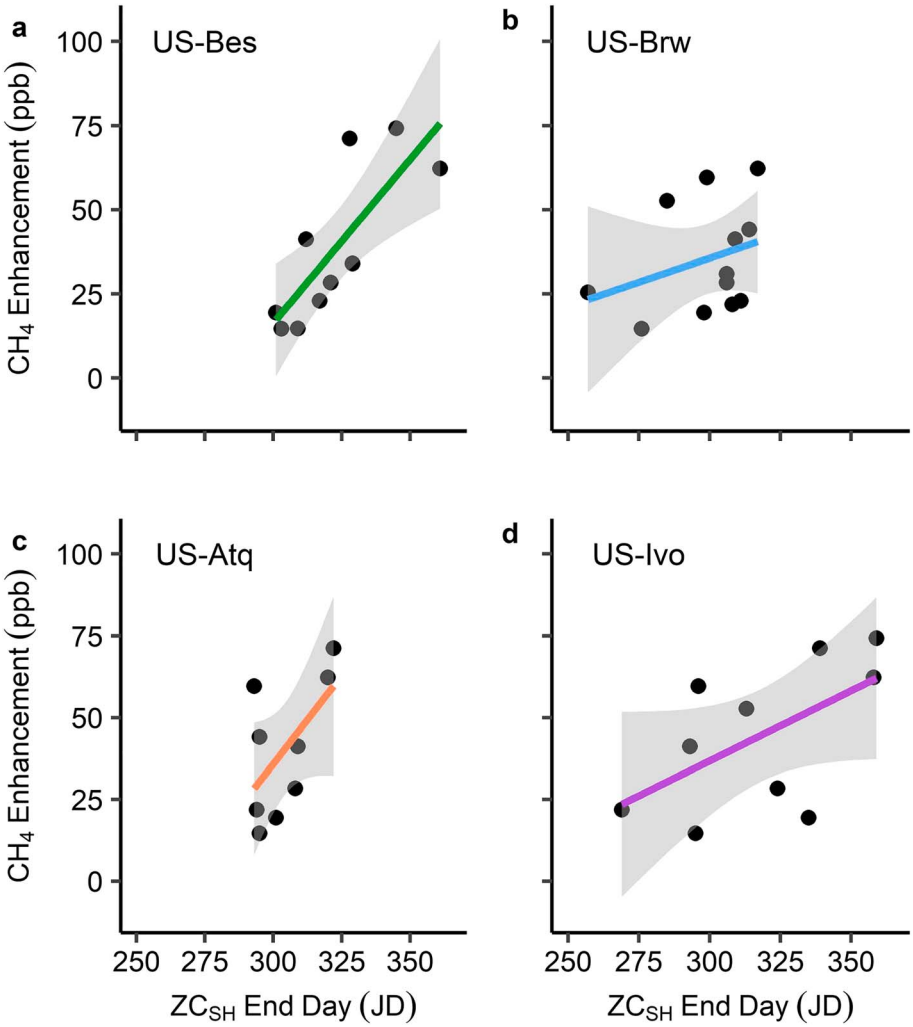

Figure 6. The fall CH_4 enhancement as a function of the ZC_{SH} end date across the four long-term sites (a, b, c, and d). LME_{CH4} was significant ($p < 0.001$, $R^2_m = 0.29$, $R^2_c = 0.29$, $N = 41$) showing an increased CH_4 enhancement with later soil freezing. Shaded region represents a 95% confidence interval. ZC = zero curtain.

gas diffusion rates (Dunfield et al., 1993), which, given low moisture content like those at the US-Atq site, support the diffusion of oxygen (Elberling et al., 2011) where methanotrophs can thrive and consume a large portion of the CH_4 produced (Zheng et al., 2018).

Our results show that the ZC_{SH} is lasting longer into the cold season over the last decades and that the ZC_F can sometimes persist well into January, after the soil surface is frozen and the air temperature is well below 0. The beginning day of the ZC_{SH} did not significantly change over the course of the study showing a one-way extension of the ZC_{SH} into the cold season. Soil moisture content is a dominant control on soil freezing considering that the development and persistence of ZC conditions are linked to latent energy released during freezing (Hinkel et al., 2001; Outcalt et al., 1990). Wetter conditions are linked to deeper thaws due to higher conductive heat transfer (Shiklomanov et al., 2010), which may further delay complete freezing given a larger active layer. Our data supports these studies in that the wetter sites generally froze on a later date than the dryer sites and that soil moisture was a significant factor in predicting when freezing may occur across the four sites.

The future of the hydrological regime in the Arctic is uncertain given differences in regional estimates of precipitation (Raynolds & Walker, 2016) and changes in drainage due to degrading permafrost that can alter water storage (Liljedahl et al., 2016). Increases in soil moisture have been observed under warming

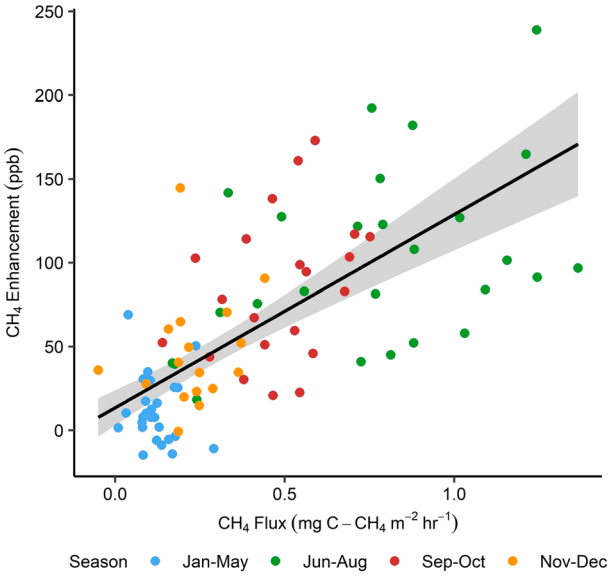

Figure 7. The weekly mean CH_4 enhancement as a function of weekly mean of CH_4 fluxes aggregated across sites showing a correlation from 2013–2017 ($p < 0.001$ and $R^2 = 0.51$, $N = 92$). A weighted generalized least squares regression (black line) was assessed. The shaded region represents a 95% confidence interval.

conditions due to soils subsiding as ice melts, bringing the surface closer to the water table (Schädel et al., 2018). Local wetting trends including general increases in wetness in high latitudes (Zhang et al., 2012) can delay soil freezing (Hinkel et al., 2001), which our results suggest could increases the fall CH_4 emissions due to the higher rates of CH_4 efflux before the soil freezes. Recent studies in more upland thermokarst regions agree with our assumptions and data as well showing a 3.5 times higher rate of CH_4 efflux under thermokarst degradation leading to wetter ecosystems (Yang et al., 2018). Therefore, we suggest that understanding and predicting hydrological changes in the Arctic is of critical importance to forecast the future of carbon budgets and specifically the role CH_4 will play with changing climate.

The joint control of CH_4 emissions by soil temperature and moisture likely explains the spatial heterogeneity in CH_4 emissions (McEwing et al., 2015; Sturtevant et al., 2012). Other studies during the Arctic fall shoulder season note a strong temperature control within one location and year but, when multiple years and sites are considered, variability in moisture content resulting from differences in precipitation, snowpack, and thawing complicates the temperature control on CH_4 emissions (Mastepanov et al., 2013). Dryer conditions can cause increased oxidation and consumption of CH_4; however, elevated CH_4 emissions are observed (Treat, Bloom, & Marushchak, 2018) during the ZC_{SH}, despite a possible reduction in moisture, showing evidence of different microbial conditions than the growing season.

Our results from the EC towers suggest continuous production and emission of CH_4 during the ZC_{SH} represented by steady sustained emissions during this time (Figure 5). Because we measured soil temperature closer to the surface, the extent of the unfrozen layer was likely still relatively large at this time and pathways to the atmosphere may be more readily available than later in the winter when a larger portion of the soil profile is frozen. The ZC_{SH} period did have relatively lower flux rates than the full growing season however as would be expected based on the temperature dependence of CH_4 production. Prior studies of CH_4 release during the ZC suggested that CH_4 trapped in frozen soils escapes suddenly in a burst through fissures in the frozen surface (Mastepanov et al., 2008;Mastepanov et al., 2013 ; Pirk et al., 2015). The bursts occur from the soil gas reserve becoming pressurized (Mastepanov et al., 2013) when soil freezes from the top-down and bottom-up as we showed in Figure 2, thanks to the high-resolution soil temperature profiles. However, these burst-like releases used the chamber flux method, which represents a small area (less than 1 m^2) of the landscape and may be better suited to observe these localized phenomena. The bursts were described as chance occurrences in space and time and were not always observed (Mastepanov et al., 2013; Pirk et al., 2015). Our results are consistent with previous EC scale studies that rarely recorded these burst emissions at the ecosystem scale and only detected them during turbulent wind events that may increase pressure gradients

Table 4
Results of LME_{soil} and LME_{air} Comparing the Ability of Soil or Air Temperature to Predict CH_4 Fluxes During the Fall

Model	df	AIC	BIC	logLik	L. ratio	*p* value	R^2_m	R^2_c
Random	3	223.94	231.90	−108.97			0	0.23
LME_{air}	4	204.27	214.89	−98.14	21.67	<0.001	0.15	0.36
LME_{soil}	4	185.47	196.08	−88.73	40.48	<0.001	0.34	0.47

Note. While both soil and air temperature are significant when compared to only the random effects, soil temperature has higher explanatory power as observed by the higher R^2. CH_4 fluxes were log transformed before performing the analysis due to the exponential response of CH_4 fluxes to temperature. *df* = degrees of freedom; AIC = Akaike information criterion; BIC = Bayesian information criterion; LME = linear mixed effect model; logLik = log of the likelihood; L. ratio = likelihood ratio compared to random model; *p* value = significance level of analysis of variance; R^2_m = correlation coefficient of the fixed variables; R^2_c = correlation coefficient of the whole model.

(Sturtevant et al., 2012; Tagesson et al., 2012; Taylor et al., 2018). In our study, CH_4 emissions may still be released through cracks in the soil and ice; however, when aggregated over the tower footprint with a shallow frozen layer, emissions were consistent and steady. Snowpack can also hold higher gas concentrations slowing the release of gases to the atmosphere (Pirk et al., 2016), which could explain why some higher fluxes have been observed during turbulent wind events in prior studies (Sturtevant et al., 2012; Tagesson et al., 2012; Taylor et al., 2018).

Studies using the NOAA ESRL tall tower data have shown that greenhouse gas terrestrial enhancements can provide important information about the controls on terrestrial CH_4 emission (Commane et al., 2017; Jeong et al., 2018; Sweeney et al., 2016). Our study shows that our EC tower CH_4 fluxes are correlated to the CH_4 enhancements estimated from the tall tower data. Importantly, the association between CH_4 flux rates, soil temperature, and CH_4 enhancements support an inferred relationship between the later ending ZC_{SH} and higher terrestrial fall CH_4 enhancements. These results imply that should the soil continue to freeze later in the year, as predicted by Euskirchen et al. (2016), more CH_4 could be released, which could contribute to climate warming.

The ZC_{SH} freezing date at US-Bes and US-Ivo were independently correlated to the CH_4 enhancement over the region. US-Bes is in a drained lake basin, a landscape feature that accounts for over 50% of the landscape of the greater Arctic Coastal Plain (Hinkel et al., 2003]. More measurements from other similar drained lake basins would be helpful to further support the representativeness of the US-Bes site of other such habitats across the Arctic Coastal Plain. Drained lake basins are inundated most of the year (Zona et al., 2009) and are composed of sedge communities (Davidson, Santos, et al., 2016) that are known to be significant emitters of CH_4 (Andresen et al., 2017; Davidson, Sloan, et al., 2016). US-Ivo, while not in a drained lake, is also on wet tundra and is also dominated by many grass and wetland vegetation (Davidson, Santos, et al., 2016). These wet environments are very conducive to CH_4 production due to anoxic conditions and the sedges aid in CH_4 transport to the atmosphere (Andresen et al., 2017; Nouchi et al., 1990; Wagner et al., 2003). The future of these habitats will likewise be important to monitor in the future to understand the variability observed in CH_4 emissions and to predict the future of the Arctic carbon balance.

As CH_4 flux measurements during the winter season are sparse (Mastepanov et al., 2008; Mastepanov et al., 2013; Pirk et al., 2015; Pirk et al., 2016; Taylor et al., 2018; Zona et al., 2016), we are only recently beginning to understand the significant contribution of the cold season to the annual Arctic carbon budget (Lüers et al., 2014; Smagin & Shnyrev, 2015; Zona et al., 2016). Methane emissions were still observed after freezing, likely due to the presence of liquid films in pore spaces (Romanovsky & Osterkamp, 2000) and cold adapted microbial communities (Wagner et al., 2003). In ecosystem-scale studies, through methods including EC towers, tall towers, and aircraft observations, the ZC period can account for over 20% of the annual CH_4 budget in Arctic ecosystems with the total cold season accounting for around 50% (Zona et al., 2016).

The high-resolution soil temperature profiles presented here show how long deeper soil temperatures may remain unfrozen (near 0 °C) while air temperatures drop to −20 to −30 °C (Figure 2). Shallower soil temperatures largely underestimated the persistence of deeper unfrozen soils up to 96 days. Even if the main transport mechanisms is stifled by upper soil layers freezing, CH_4 production may still be occurring below the surface and could be released in bursts (Mastepanov et al., 2008; Pirk et al., 2015) or after spring thaw (Pirk et al., 2017). Our results suggest that CH_4 emissions are decoupled from air temperature especially in the fall shoulder season, consistent with previous work (Byun et al., 2017) and with the understanding that CH_4 is largely produced in anoxic soil layers below the surface (Lai, 2009; Treat et al., 2015; Zehnder, 1978). The lack of correlation between the terrestrial fall CH_4 enhancement and air temperatures agree with prior studies (Sweeney et al., 2016) and emphasizes the disconnect between above and below surface conditions and the importance of the persistence of unfrozen soil layers.

Arctic tundra CH_4 emissions are currently minor compared to larger natural CH_4 sources including tropical wetlands (15% of wetland CH_4 emissions originate from Boreal and Arctic ecosystems (Kirschke et al., 2013)); however, given large soil carbon storage, their contribution could increase with anticipated warming (Schuur et al., 2013) and the increased wetness in the Arctic Coastal Plain of Alaska (Raynolds & Walker, 2016).

5. Conclusions

This study shows that long-term records of soil temperature, moisture, CH_4 concentrations, and CH_4 fluxes are essential to accurately predicting the impact of warming on the Arctic CH_4 budget. Soils are freezing later into the cold season, and the persistence of unfrozen soils later into the fall can sustain higher CH_4 emissions. As the Arctic continues to warm, positive feedbacks such as increased CH_4 emissions linked to a later soil freezing may occur. The air temperature and even the surface soil temperature are unable to capture the persistence of deeper unfrozen soil layers, underestimating the duration of the ZC_F by over 2 months in some cases.

To further confirm the hypothesized role of later soil freezing to the terrestrial fall CH_4 enhancement, a more continuous and wider-spread isotopic analysis of the CH_4 in the soil and atmosphere should be collected across the Arctic. This could help identify the timing and relative contribution of CH_4 sources (Fisher et al., 2017). Including cold season CH_4 emissions into models will improve estimates of the annual CH_4 budget (Warwick et al., 2016), especially with the importance of later soil freezing on atmospheric CH_4 concentrations. Future studies should also identify the soil layers responsible for the fall CH_4 production and consumption, and the direct mechanisms controlling CH_4 release during the entire ZC and greater cold period. This understanding is critical for refining predictions of the sensitivity of CH_4 emissions to increasing permafrost degradation in the Arctic. Spatially widespread observations are also critical since habitat heterogeneity is an important factor in carbon cycling dynamics (Davidson, Sloan, et al., 2016; Treat, Marushchak, et al., 2018). Gas concentration, isotopic analyses, and CH_4 flux measurements within the soil column could identify locations of methanogenesis and CH_4 oxidation, as well as the processes responsible for the potential CH_4emission when the upper soil layers start to freeze. The results of this study emphasize that increased attention should be placed on cold season soil conditions to properly constrain predictions of Arctic annual carbon budgets.

Acknowledgments
Flux and meteorological data from the flux towers are available through the AmeriFlux data portal and NOAA data are available through the NOAA ESRL data portal (https://www.esrl.noaa.gov/gmd/dv/data/index.php?site=BRW). Funding for AmeriFlux data resources was provided by the U.S. Department of Energy's Office of Science. High-resolution temperature data are available from the NSF Arctic Data Center (doi:10.18739/A25X25C75). This work was funded by the Office of Polar Programs (OPP) of the National Science Foundation (NSF) awarded to D. Z., W. C. O., and D. A. L. (awards 1204263 and 1702797) with additional logistical support funded by the NSF Office of Polar Programs, by the Carbon in Arctic Reservoirs Vulnerability Experiment (CARVE), an Earth Ventures (EV-1) investigation, under contract with the National Aeronautics and Space Administration, and by the ABoVE (NNX15AT74A, NNX16AF94A, and NNX17AC61A) Program. Additional support was provided by NOAA Cooperative Science Center for Earth System Sciences and Remote Sensing Technologies (NOAA-CESSRST) under the Cooperative Agreement Grant NA16SEC4810008. This research was conducted on land owned by the Ukpeaġvik Inupiat Corporation (UIC) whom we would like to thank for their continued support. This project has received funding from the European Union's Horizon 2020 research and innovation program under Grant agreement 727890 and from the Natural Environment Research Council (NERC) UAMS Grant (NE/P002552/1). Geospatial support for this work provided by the Polar Geospatial Center under NSF OPP awards 1204263 and 1702797. Authors would additionally like to thank the R developing team (R core team, Vienna, Austria) for their part in creating the open source R statistical software.

References

Andresen, C. G., Lara, M. J., Tweedie, C. E., & Lougheed, V. L. (2017). Rising plant-mediated methane emissions from arctic wetlands. *Global Change Biology*, *23*(3), 1128–1139. https://doi.org/10.1111/gcb.13469

Arndt, K., Zona, D., Hashemi, J., Kalhori, A. A. M., & Oechel, W. (2019). High resolution temperature profiles along a latitudinal gradient near Utqiagvik, Atqasuk, and Ivotuk Alaska from 2016-2019. Retrieved from: https://doi.org/10.18739/A25X25C75

Barton, K. (2018). MuMIn: Multi-Model Inference.

Bekryaev, R. V., Polyakov, I. V., & Alexeev, V. A. (2010). Role of polar amplification in long-term surface air temperature variations and modern Arctic warming. *Journal of Climate*, *23*(14), 3888–3906. https://doi.org/10.1175/2010jcli3297.1

Bivand, R., Keitt, T., & Rowlingson, B. (2018). rgdal: Bindings for the 'Geospatial' Data Abstraction Library.

Byun, E., Yang, J.-W., Kim, Y., & Ahn, J. (2017). Trapped greenhouse gases in the permafrost active layer: Preliminary results for methane peaks in vertical profiles of frozen Alaskan soil cores. *Permafrost and Periglacial Processes*, *28*(2), 477–484. https://doi.org/10.1002/ppp.1935

Carroll, R. J. (2017). *Transformation and weighting in regression*. New York: Routledge.

Carroll, R. J., & Ruppert, D. (1982). A comparison between maximum likelihood and generalized least squares in a heteroscedastic linear model. *Journal of the American Statistical Association*, *77*(380), 878–882. https://doi.org/10.1080/01621459.1982.10477901

Commane, R., Lindaas, J., Benmergui, J., Luus, K. A., Chang, R. Y. W., Daube, B. C., et al. (2017). Carbon dioxide sources from Alaska driven by increasing early winter respiration from Arctic tundra. *Proceedings of the National Academy of Sciences of the United States of America*, *114*(21), 5361–5366. https://doi.org/10.1073/pnas.1618567114

Crill, P. M., & Thornton, B. F. (2017). Whither methane in the IPCC process? *Nature Climate Change*, *7*(10), 678–680. https://doi.org/10.1038/nclimate3403

Davidson, S. J., Santos, M. J., Sloan, V. L., Watts, J. D., Phoenix, G. K., Oechel, W. C., & Zona, D. (2016). Mapping Arctic tundra vegetation communities using field spectroscopy and multispectral satellite data in North Alaska, USA. *Remote Sensing*, *8*(12). https://doi.org/10.3390/rs8120978

Davidson, S. J., Sloan, V. L., Phoenix, G. K., Wagner, R., Fisher, J. P., Oechel, W. C., & Zona, D. (2016). Vegetation type dominates the spatial variability in CH_4 emissions across multiple Arctic tundra landscapes. *Ecosystems*, *19*(6), 1116–1132. https://doi.org/10.1007/s10021-016-9991-0

Dunfield, P., Knowles, R., Dumont, R., & Moore, T. R. (1993). Methane production and consumption in temperate and subarctic peat soils: Response to temperature and pH. *Soil Biology and Biochemistry*, *25*(3), 321–326. https://doi.org/10.1016/0038-0717(93)90130-4

Dunnington, D. (2017). prettymapr: Scale bar, north arrow, and pretty margins in R.

Elberling, B., Askaer, L., Jørgensen, C. J., Joensen, H. P., Kühl, M., Glud, R. N., & Lauritsen, F. R. (2011). Linking soil O_2, CO_2, and CH_4 concentrations in a Wetland soil: Implications for CO_2 and CH_4 fluxes. *Environmental Science & Technology*, *45*(8), 3393–3399. https://doi.org/10.1021/es103540k

Elberling, B., & Brandt, K. K. (2003). Uncoupling of microbial CO_2 production and release in frozen soil and its implications for field studies of arctic C cycling. *Soil Biology and Biochemistry*, *35*(2), 263–272. https://doi.org/10.1016/S0038-0717(02)00258-4

Euskirchen, E. S., Bret-Harte, M. S., Shaver, G. R., Edgar, C. W., & Romanovsky, V. E. (2016). Long-term release of carbon dioxide from Arctic tundra ecosystems in Alaska. *Ecosystems*, *20*(5), 960–974. https://doi.org/10.1007/s10021-016-0085-9

Fisher, R. E., France, J. L., Lowry, D., Lanoisellé, M., Brownlow, R., Pyle, J. A., et al. (2017). Measurement of the ^{13}C isotopic signature of methane emissions from northern European wetlands. *Global Biogeochemical Cycles*, *31*, 605–623. https://doi.org/10.1002/2016GB005504

Freitag, T. E., Toet, S., Ineson, P., & Prosser, J. I. (2010). Links between methane flux and transcriptional activities of methanogens and methane oxidizers in a blanket peat bog. *FEMS Microbiology Ecology*, *73*(1), 157–165. https://doi.org/10.1111/j.1574-6941.2010.00871.x

Goodrich, J. P., Oechel, W. C., Gioli, B., Moreaux, V., Murphy, P. C., Burba, G., & Zona, D. (2016). Impact of different eddy covariance sensors, site set-up, and maintenance on the annual balance of CO_2 and CH_4 in the harsh Arctic environment. *Agricultural and Forest Meteorology*, *228-229*, 239–251. https://doi.org/10.1016/j.agrformet.2016.07.008

Hijmans, R. J. (2018). raster: Geographic data analysis and modeling.

Hinkel, K. M., Eisner, W. R., Bockheim, J. G., Nelson, F. E., Peterson, K. M., & Dai, X. (2003). Spatial extent, age, and carbon stocks in drained thaw lake basins on the Barrow Peninsula, Alaska. *Arctic, Antarctic, and Alpine Research*, *35*(3), 291–300. https://doi.org/10.1657/1523-0430(2003)035[0291:Seaacs]2.0.Co;2

Hinkel, K. M., Paetzold, F., Nelson, F. E., & Bockheim, J. G. (2001). Patterns of soil temperature and moisture in the active layer and upper permafrost at Barrow, Alaska: 1993–1999. *Global and Planetary Change*, *29*(3-4), 293–309. https://doi.org/10.1016/S0921-8181(01)00096-0

Ho, A., de Roy, K., Thas, O., de Neve, J., Hoefman, S., Vandamme, P., et al. (2014). The more, the merrier: Heterotroph richness stimulates methanotrophic activity. *The ISME Journal*, *8*(9), 1945–1948. https://doi.org/10.1038/ismej.2014.74

Hugelius, G., Strauss, J., Zubrzycki, S., Harden, J. W., Schuur, E. A. G., Ping, C. L., et al. (2014). Estimated stocks of circumpolar permafrost carbon with quantified uncertainty ranges and identified data gaps. *Biogeosciences*, *11*(23), 6573–6593. https://doi.org/10.5194/bg-11-6573-2014

Ibrom, A., Dellwik, E., Flyvbjerg, H., Jensen, N. O., & Pilegaard, K. (2007). Strong low-pass filtering effects on water vapour flux measurements with closed-path eddy correlation systems. *Agricultural and Forest Meteorology*, *147*(3-4), 140–156. https://doi.org/10.1016/j.agrformet.2007.07.007

IPCC. (2013). Climate change 2013: The physical science basis. Contribution of Working Group I to the Fifth Assessment Report of the Intergovernmental Panel on Climate Change. UK and New York.

Jeong, S.-J., Bloom, A. A., Schimel, D., Sweeney, C., Parazoo, N. C., Medvigy, D., et al. (2018). Accelerating rates of Arctic carbon cycling revealed by long-term atmospheric CO_2 measurements. *Science Advances*, *4*(7). https://doi.org/10.1126/sciadv.aao1167

Kirschke, S., Bousquet, P., Ciais, P., Saunois, M., Canadell, J. G., Dlugokencky, E. J., et al. (2013). Three decades of global methane sources and sinks. *Nature Geoscience*, *6*(10), 813–823. https://doi.org/10.1038/ngeo1955

Kormann, R., & Meixner, F. X. (2001). An analytical footprint model for non-neutral stratification. *Boundary-Layer Meteorology*, *99*(2), 207–224. https://doi.org/10.1023/A:1018991015119

Kwon, H.-J., Oechel, W. C., Zulueta, R. C., & Hastings, S. J. (2006). Effects of climate variability on carbon sequestration among adjacent wet sedge tundra and moist tussock tundra ecosystems. *Journal of Geophysical Research*, *111*, G03014. https://doi.org/10.1029/2005JG000036

Lai, D. Y. F. (2009). Methane dynamics in northern peatlands: A review. *Pedosphere*, *19*(4), 409–421. https://doi.org/10.1016/S1002-0160(09)00003-4

Liljedahl, A. K., Boike, J., Daanen, R. P., Fedorov, A. N., Frost, G. V., Grosse, G., et al. (2016). Pan-Arctic ice-wedge degradation in warming permafrost and its influence on tundra hydrology. *Nature Geoscience*, *9*(4), 312–318. https://doi.org/10.1038/ngeo2674

Lipson, D. A., Haggerty, J. M., Srinivas, A., Raab, T. K., Sathe, S., & Dinsdale, E. A. (2013). Metagenomic insights into anaerobic metabolism along an Arctic peat soil profile. *PLoS ONE*, *8*(5), e64659. https://doi.org/10.1371/journal.pone.0064659

Lüers, J., Westermann, S., Piel, K., & Boike, J. (2014). Annual CO_2 budget and seasonal CO_2 exchange signals at a high Arctic permafrost site on Spitsbergen, Svalbard archipelago. *Biogeosciences*, *11*(22), 6307–6322. https://doi.org/10.5194/bg-11-6307-2014

Mastepanov, M., Sigsgaard, C., Dlugokencky, E. J., Houweling, S., Strom, L., Tamstorf, M. P., & Christensen, T. R. (2008). Large tundra methane burst during onset of freezing. *Nature*, *456*(7222), 628–630. https://doi.org/10.1038/nature07464

Mastepanov, M., Sigsgaard, C., Tagesson, T., Ström, L., Tamstorf, M. P., Lund, M., & Christensen, T. R. (2013). Revisiting factors controlling methane emissions from high-Arctic tundra. *Biogeosciences*, *10*(7), 5139–5158. https://doi.org/10.5194/bg-10-5139-2013

Mauder, M., & Foken, T. (2011). Documentation and instruction manual of the eddy-covariance software package TK3. In (Vol. 46). Bayreuth.

McEwing, K. R., Fisher, J. P., & Zona, D. (2015). Environmental and vegetation controls on the spatial variability of CH_4 emission from wet-sedge and tussock tundra ecosystems in the Arctic. *Plant and Soil*, *388*(1-2), 37–52. https://doi.org/10.1007/s11104-014-2377-1

McLain, J. E. T., Kepler, T. B., & Ahmann, D. M. (2002). Belowground factors mediating changes in methane consumption in a forest soil under elevated CO_2. *Global Biogeochemical Cycles*, *16*(3), 1050. https://doi.org/10.1029/2001GB001439

Moncrieff, J., Clement, R., Finnigan, J., & Meyers, T. (2005). Averaging, detrending, and filtering of eddy covariance time series. In X. Lee, W. Massman, & B. Law (Eds.), *Handbook of micrometeorology: A guide for surface flux measurement and analysis* (pp. 7–31). Dordrecht, Netherlands: Springer. https://doi.org/10.1007/1-4020-2265-4_2

Moncrieff, J. B., Massheder, J. M., de Bruin, H., Elbers, J., Friborg, T., Heusinkveld, B., et al. (1997). A system to measure surface fluxes of momentum, sensible heat, water vapour and carbon dioxide. *Journal of Hydrology*, *188-189*, 589–611. https://doi.org/10.1016/S0022-1694(96)03194-0

Murrell, P. (2014). gridBase: Integration of base and grid graphics.

Nakagawa, S., Johnson, P. C. D., & Schielzeth, H. (2017). The coefficient of determination R(2) and intra-class correlation coefficient from generalized linear mixed-effects models revisited and expanded. *Journal of the Royal Society Interface*, *14*(134). https://doi.org/10.1098/rsif.2017.0213

Nazaries, L., Murrell, J. C., Millard, P., Baggs, L., & Singh, B. K. (2013). Methane, microbes and models: Fundamental understanding of the soil methane cycle for future predictions. *Environmental Microbiology*, *15*(9), 2395–2417. https://doi.org/10.1111/1462-2920.12149

Nisbet, E. G., Dlugokencky, E. J., Manning, M. R., Lowry, D., Fisher, R. E., France, J. L., et al. (2016). Rising atmospheric methane: 2007-2014 growth and isotopic shift. *Global Biogeochemical Cycles*, *30*, 1356–1370. https://doi.org/10.1002/2016GB005406

Nouchi, I., Mariko, S., & Aoki, K. (1990). Mechanism of methane transport from the rhizosphere to the atmosphere through rice plants. *Plant Physiology*, *94*(1), 59–66. https://doi.org/10.1104/pp.94.1.59

Outcalt, S. I., Nelson, F. E., & Hinkel, K. M. (1990). The zero-curtain effect: Heat and mass transfer across an isothermal region in freezing soil. *Water Resources Research*, *26*(7), 1509–1516. https://doi.org/10.1029/WR026i007p01509

Pinheiro, J., & Bates, D. (2000). *Mixed-effects models in S and S-PLUS*. New York, NY: Springer. https://doi.org/10.1007/978-1-4419-0318-1

Pinheiro, J., Bates, D., DebRoy, S., Sarkar, D., & Team, R. C. (2018). nlme: Linear and nonlinear mixed effects models.

Pirk, N., Mastepanov, M., López-Blanco, E., Christensen, L. H., Christiansen, H. H., Hansen, B. U., et al. (2017). Toward a statistical description of methane emissions from arctic wetlands. *Ambio*, *46*(Suppl 1), 70–80. https://doi.org/10.1007/s13280-016-0893-3

Pirk, N., Santos, T., Gustafson, C., Johansson, A. J., Tufvesson, F., Parmentier, F.-J. W., et al. (2015). Methane emission bursts from permafrost environments during autumn freeze-in: New insights from ground-penetrating radar. *Geophysical Research Letters*, *42*, 6732–6738. https://doi.org/10.1002/2015GL065034

Pirk, N., Tamstorf, M. P., Lund, M., Mastepanov, M., Pedersen, S. H., Mylius, M. R., et al. (2016). Snowpack fluxes of methane and carbon dioxide from high Arctic tundra. *Journal of Geophysical Research: Biogeosciences*, *121*, 2886–2900. https://doi.org/10.1002/2016JG003486

Poulter, B., Bousquet, P., Canadell, J. G., Ciais, P., Peregon, A., Saunois, M., et al. (2017). Global wetland contribution to 2000–2012 atmospheric methane growth rate dynamics. *Environmental Research Letters*, *12*(9). https://doi.org/10.1088/1748-9326/aa8391

R Core Team. (2018). R: A language and environment for statistical computing. In.

Raynolds, M. K., & Walker, D. A. (2016). Increased wetness confounds Landsat-derived NDVI trends in the central Alaska North Slope region, 1985–2011. *Environmental Research Letters*, *11*(8). https://doi.org/10.1088/1748-9326/11/8/085004

Reichstein, M., Falge, E., Baldocchi, D., Papale, D., Aubinet, M., Berbigier, P., et al. (2005). On the separation of net ecosystem exchange into assimilation and ecosystem respiration: Review and improved algorithm. *Global Change Biology*, *11*(9), 1424–1439. https://doi.org/10.1111/j.1365-2486.2005.001002.x

Romanovsky, V. E., & Osterkamp, T. E. (2000). Effects of unfrozen water on heat and mass transport processes in the active layer and permafrost. *Permafrost and Periglacial Processes*, *11*(3), 219–239. https://doi.org/10.1002/1099-1530(200007/09)11:3<219::AID-PPP352>3.0.CO;2-7

Saunois, M., Jackson, R. B., Bousquet, P., Poulter, B., & Canadell, J. G. (2016). The growing role of methane in anthropogenic climate change. *Environmental Research Letters*, *11*(12). https://doi.org/10.1088/1748-9326/11/12/120207

Schädel, C., Koven, C. D., Lawrence, D. M., Celis, G., Garnello, A. J., Hutchings, J., et al. (2018). Divergent patterns of experimental and model-derived permafrost ecosystem carbon dynamics in response to Arctic warming. *Environmental Research Letters*, *13*(10). https://doi.org/10.1088/1748-9326/aae0ff

Schuur, E. A. G., Abbott, B. W., Bowden, W. B., Brovkin, V., Camill, P., Canadell, J. G., et al. (2013). Expert assessment of vulnerability of permafrost carbon to climate change. *Climatic Change*, *119*(2), 359–374. https://doi.org/10.1007/s10584-013-0730-7

Schuur, E. A. G., McGuire, A. D., Schädel, C., Grosse, G., Harden, J. W., Hayes, D. J., et al. (2015). Climate change and the permafrost carbon feedback. *Nature*, *520*(7546), 171–179. https://doi.org/10.1038/nature14338

Shiklomanov, N. I., Streletskiy, D. A., Nelson, F. E., Hollister, R. D., Romanovsky, V. E., Tweedie, C. E., et al. (2010). Decadal variations of active-layer thickness in moisture-controlled landscapes, Barrow, Alaska. *Journal of Geophysical Research*, *115*, G00I04. https://doi.org/10.1029/2009JG001248

Smagin, A. V., & Shnyrev, N. A. (2015). Methane fluxes during the cold season: Distribution and mass transfer in the snow cover of bogs. *Eurasian Soil Science*, *48*(8), 823–830. https://doi.org/10.1134/s1064229315080086

Sturtevant, C. S., Oechel, W. C., Zona, D., Kim, Y., & Emerson, C. E. (2012). Soil moisture control over autumn season methane flux, Arctic Coastal Plain of Alaska. *Biogeosciences*, *9*(4), 1423–1440. https://doi.org/10.5194/bg-9-1423-2012

Sweeney, C., Dlugokencky, E., Miller, C. E., Wofsy, S., Karion, A., Dinardo, S., et al. (2016). No significant increase in long-term CH_4 emissions on North Slope of Alaska despite significant increase in air temperature. *Geophysical Research Letters*, *43*, 6604–6611. https://doi.org/10.1002/2016GL069292

Tagesson, T., Mölder, M., Mastepanov, M., Sigsgaard, C., Tamstorf, M. P., Lund, M., et al. (2012). Land-atmosphere exchange of methane from soil thawing to soil freezing in a high-Arctic wet tundra ecosystem. *Global Change Biology*, *18*(6), 1928–1940. https://doi.org/10.1111/j.1365-2486.2012.02647.x

Taylor, M. A., Celis, G., Ledman, J. D., Bracho, R., & Schuur, E. A. G. (2018). Methane efflux measured by eddy covariance in Alaskan upland tundra undergoing permafrost degradation. *Journal of Geophysical Research: Biogeosciences*, *123*, 2695–2710. https://doi.org/10.1029/2018JG004444

Treat, C. C., Bloom, A. A., & Marushchak, M. E. (2018). Nongrowing season methane emissions—A significant component of annual emissions across northern ecosystems. *Global Change Biology*, *24*(8), 3331–3343. https://doi.org/10.1111/gcb.14137

Treat, C. C., Marushchak, M. E., Voigt, C., Zhang, Y., Tan, Z., Zhuang, Q., et al. (2018). Tundra landscape heterogeneity, not interannual variability, controls the decadal regional carbon balance in the Western Russian Arctic. *Global Change Biology*, *24*(11), 5188–5204. https://doi.org/10.1111/gcb.14421

Treat, C. C., Natali, S. M., Ernakovich, J., Iversen, C. M., Lupascu, M., McGuire, A. D., et al. (2015). A pan-Arctic synthesis of CH_4 and CO_2 production from anoxic soil incubations. *Global Change Biology*, *21*(7), 2787–2803. https://doi.org/10.1111/gcb.12875

Tucker, C. (2014). Reduction of air- and liquid water-filled soil pore space with freezing explains high temperature sensitivity of soil respiration below 0 °C. *Soil Biology and Biochemistry*, *78*, 90–96. https://doi.org/10.1016/j.soilbio.2014.06.018

Wagner, D., Kobabe, S., Pfeiffer, E. M., & Hubberten, H. W. (2003). Microbial controls on methane fluxes from a polygonal tundra of the Lena Delta, Siberia. *Permafrost and Periglacial Processes*, *14*(2), 173–185. https://doi.org/10.1002/ppp.443

Wagner, R., Zona, D., Oechel, W., & Lipson, D. (2017). Microbial community structure and soil pH correspond to methane production in Arctic Alaska soils. *Environmental Microbiology*, *19*(8), 3398–3410. https://doi.org/10.1111/1462-2920.13854

Walker, D. A., Binnian, E. F., Evans, B. M., Lederer, N. D., Nordstrand, E. A., & Webber, P. J. (1989). Terrain, vegetation, and landscape evolution of the R4D research site, Brooks Range Foothills, Alaska. *Holarctic Ecology*, *12*(3), 238–261.

Warwick, N. J., Cain, M. L., Fisher, R., France, J. L., Lowry, D., Michel, S. E., et al. (2016). Using $\delta^{13}C$-CH_4 and δD-CH_4 to constrain Arctic methane emissions. *Atmospheric Chemistry and Physics*, *16*(23), 14,891–14,908. https://doi.org/10.5194/acp-16-14891-2016

Webb, E. K., Pearman, G. I., & Leuning, R. (1980). Correction of flux measurements for density effects due to heat and water vapour transfer. *Quarterly Journal of the Royal Meteorological Society*, *106*(447), 85–100. https://doi.org/10.1002/qj.49710644707

Wilczak, J. M., Oncley, S. P., & Stage, S. A. (2001). Sonic anemometer tilt correction algorithms. *Boundary-Layer Meteorology*, *99*(1), 127–150. https://doi.org/10.1023/a:1018966204465

Xenakis, G. (2016). FREddyPro: Post-processing EddyPro full output file. R package version 1.0.

Yang, G., Peng, Y., Olefeldt, D., Chen, Y., Wang, G., Li, F., et al. (2018). Changes in methane flux along a permafrost thaw sequence on the Tibetan Plateau. *Environmental Science & Technology*, *52*(3), 1244–1252. https://doi.org/10.1021/acs.est.7b04979

Yavitt, J. B., Yashiro, E., Cadillo-Quiroz, H., & Zinder, S. H. (2011). Methanogen diversity and community composition in peatlands of the central to northern Appalachian Mountain region, North America. *Biogeochemistry*, *109*(1-3), 117–131. https://doi.org/10.1007/s10533-011-9644-5

Zehnder, A. J. B. (1978). In R. Mitchell (Ed.), *Ecology of methane formation* (Vol. 2). New York: Wiley.

Zhang, X., He, J., Zhang, J., Polyakov, I., Gerdes, R., Inoue, J., & Wu, P. (2012). Enhanced poleward moisture transport and amplified northern high-latitude wetting trend. *Nature Climate Change*, *3*(1), 47–51. https://doi.org/10.1038/nclimate1631

Zhang, Z., Zimmermann, N. E., Stenke, A., Li, X., Hodson, E. L., Zhu, G., et al. (2017). Emerging role of wetland methane emissions in driving 21st century climate change. *Proceedings of the National Academy of Sciences of the United States of America*, *114*(36), 9647–9652. https://doi.org/10.1073/pnas.1618765114

Zheng, J., RoyChowdhury, T., Yang, Z., Gu, B., Wullschleger, S. D., & Graham, D. E. (2018). Impacts of temperature and soil characteristics on methane production and oxidation in Arctic tundra. *Biogeosciences*, *15*(21), 6621–6635. https://doi.org/10.5194/bg-15-6621-2018

Zona, D., Gioli, B., Commane, R., Lindaas, J., Wofsy, S. C., Miller, C. E., et al. (2016). Cold season emissions dominate the Arctic tundra methane budget. *Proceedings of the National Academy of Sciences of the United States of America*, *113*(1), 40–45. https://doi.org/10.1073/pnas.1516017113

Zona, D., & Oechel, W. (1999). Ameriflux US-Atq Atqasuk. https://doi.org/10.17190/AMF/1246029

Zona, D., & Oechel, W. (1998). AmeriFlux US-Brw Barrow. https://doi.org/10.17190/AMF/1246041

Zona, D., & Oechel, W. (2003). AmeriFlux US-Ivo Ivotuk. https://doi.org/10.17190/AMF/1246067

Zona, D., Oechel, W. C., Kochendorfer, J., Paw U, K. T., Salyuk, A. N., Olivas, P. C., et al. (2009). Methane fluxes during the initiation of a large-scale water table manipulation experiment in the Alaskan Arctic tundra. *Global Biogeochemical Cycles*, *23*, GB2013. https://doi.org/10.1029/2009GB003487